THE AMERICAN MINERALOGIST, VOL. 46, NOVEMBER–DECEMBER, 1961

LIGHT SCATTERING FROM HEAT TREATED SYNTHETIC QUARTZ

J. A. BASTIN* AND E. W. J. MITCHELL, *J. J. Thomson Physical Laboratory, The University, Reading.*

ABSTRACT

Many crystal plates of synthetic quartz appear milky after heating above about 650° C. In some specimens individual scattering particles can be resolved and are found to lie on planes, some of which (*e.g.* (00.1)) are crystallographically simple. In most specimens the scattering particles are grouped in more or less well-defined macroscopic regions. In a particular group of specimens these regions are well defined hexagonal prisms parallel to the *c*-axis. Before heat treatment it was shown that these prismatic regions were colored by ionizing radiation showing the well known broad band at about 4500 Å believed to be associated with Al impurity. Direct spectrographic analysis also showed that those specimens which contained most Al would have the highest light scattering coefficient after heat treatment.

The kinetics of the formation of the scattering particles was studied and the formation of the particles is limited by an activated process of energy 1.1 ± 0.1 eV.

A model is put forward to account for the results. It is suggested that the scattering particles result from the precipitation of Al which diffuses interstitially through the crystal to precipitation centers. These centers are frequently localized on planes; such centers might result from the intersection of edge dislocations with laminar faults.

INTRODUCTION

During experiments on the annealing of radiation damage in quartz it was noticed that synthetic specimens were invariably "milky" after heating above about 650° C. This effect was not found with natural (Brazilian) quartz. Subsequently an investigation was carried out of the conditions of formation of the scattering centers and of their spatial distribution. The results are described in this paper.

EXPERIMENTAL

The quartz crystals were grown by the hydrothermal method by the G.E.C., Wembley, England, and by Sawyer Products Inc., Cleveland, U.S.A. The G.E.C. crystals (see, for example, Brown and Thomas 1956) were grown on seeds in the form of plates cut perpendicular to the *c*-axis. The American crystals (see, for example, Bechmann & Hale 1955) were grown on long narrow bars of rectangular cross section. The long axis of each bar was parallel to the *y*-axis while the long narrow faces were perpendicular to either the *a*- or the *c*-axis. The G.E.C. supplied three types of crystals, differing in the amounts of Al impurity which had been incorporated. We refer to these as G I, G II and G III, and according to spectrographic analysis carried out by the G.E.C., the approximate concentrations of Al are as given in Table I.

* Now at Physics Department, Queen Mary College, London.

The specimens were heated in air in a temperature controlled silica tube furnace. It was found necessary, for plates of thickness greater than about 1.5 mm., to heat and cool slowly (1° per min.) in order to avoid cracking the specimens. For this reason the controller was fitted with an automatic drive and a given heat treatment was programmed with a specially cut cam. From time to time a chromel-alumel thermocouple was used to measure the temperature adjacent to the specimen. This temperature was found to be within 5° of that shown on the controller.

After heat treatment the crystals were examined with three kinds of microscopes:

(1) Low power (up to ×60).

(2) Leitz "ultramicroscope," which is a device for viewing light scattered at right angles to the incident beam. The scattered light was viewed through a low power microscope (up to ×60).

TABLE I

Type	Estimated weight % of Al	Mean Σ cm.$^{-1}$ defined	No. of specimens investigated for determination of Σ
G I	10^{-3}	7.2 ± 3	6
G II	$5-10 \times 10^{-3}$	38 ± 15	5
G III	2×10^{-2}	64	1

(3) Vickers projection microscope using a 4 mm. dark-field illumination objective to give magnifications on the screen of 1000. The fine adjustment head allowed the height of the specimen to be varied and set to 10^{-5} cm. The stage could be moved, by micrometers, in two perpendicular horizontal directions.

The spectral transmission of the specimens before and after heat treatment was measured with a Hilger Uvispek spectrophotometer. Measurements were also made using an integrating sphere in conjunction with the spetrophotometer as described by Bastin *et al.* (1959). In the former case light is removed from the straight-through beam by scattering and absorption, while in the integrating sphere the only losses recorded arise from absorption. Combining the two sets of data it is possible to separate scattering and absorption effects.

The Distribution of Scattering Centers

All regions of the G.E.C. specimens and some regions of the Sawyer specimens were found to be permanently milky after heating above 650° C. The distribution of milkiness in the various specimens was as follows:

G.E.C. Type G I

Plates of thickness 0.05 cm. cut perpendicular to the *c*-axis showed an irregularly mottled appearance. Some unheated specimens were irradiated in the Harwell pile BEPO (1.7×10^{18} $n°$ cm^{-2}) and the induced smoky color was distributed in a similarly irregular way. However, in one case when the heat treatment was carried out on an irradiated specimen there was no obvious spatial correlation between the irradiation coloring and scattering patterns. Plates cut at right angles to a Y direction showed macroscopic striations in the basal plane. Similarly orientated striations were found in pile irradiated crystals of this type although the regions of preferentially dense radiation coloring tended to become regions of lower scattering power.

G.E.C. Type G II

Specimens cut parallel to the basal plane and viewed in the direction of the *c*-axis showed well-defined regions containing a preferentially high density of scattering centers. Fig. 1*a* shows a photograph taken with the Leitz ultra-microscope in which the regions appear in the form of equilateral triangles with the corners cut off by intersection with larger equilateral triangles. When the focal plane was moved through the

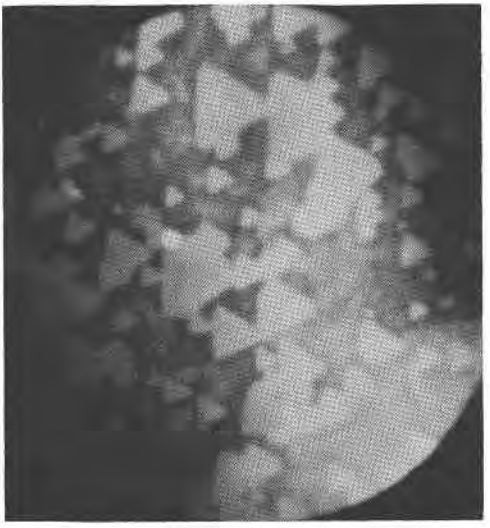

(*a*)

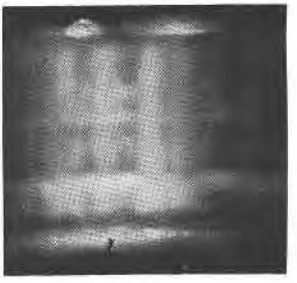

(*b*)

FIG. 1. Photographs of specimen G II_2 taken by scattered light with a Leitz ultra-microscope viewed (*a*) in the *c*-axis direction (55×), and (*b*) at right angles to the *c*-axis, which is vertical (40×).

specimen in the direction of the c-axis the "triangles" remained in focus through most of the thickness of the specimen. This suggested that a high density of scattering centers existed within "triangular" *prisms* whose axes were parallel to the c-axis. Confirmation of this can be seen in Fig. 1*b* which shows a photograph taken by scattered light of the same specimen viewed in a direction at right angles to the c-axis. The prisms are now seen as striations. If the focal plane was lowered or raised the striations were found to remain in focus for a distance of about 0.01–0.02 cm. As the striations disappeared other randomly positioned

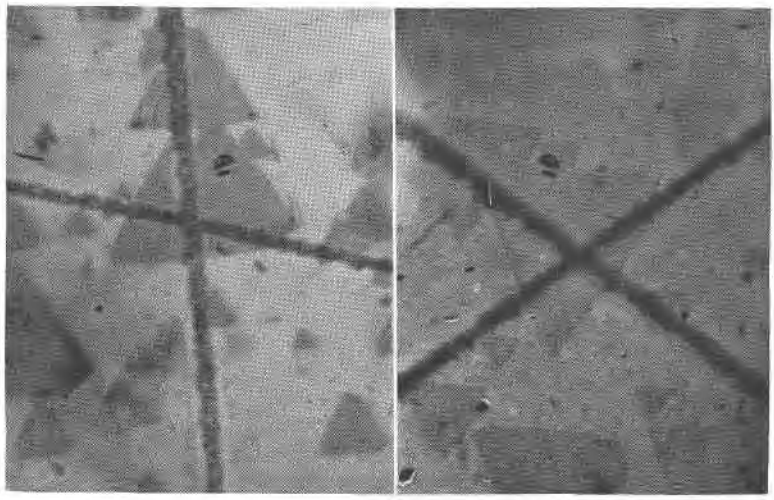

(*a*) (*b*)

FIG. 2. Photographs of specimen G II_2 taken by transmitted light (*a*) after neutron irradiation (1.7×10^{18} $n°$ cm.$^{-2}$). 85×; (*b*) after subsequent heating at 700° C. for 24 hours. 77×.

but parallel striations came into focus. This is consistent with the presence of prisms of cross-section dimensions of about 0.01–0.02 cm. (as indicated by Fig. 1*a*), randomly distributed in a basal plane but all parallel to the c-axis. Back reflection Laue photographs showed that, contrary to what might be expected, the directions of the "triangular" edges of the cross-section of the prisms do not coincide with a-axes. In the specimen examined these edges were at an angle of 13°.

The following experiment was carried out to see whether there was any correlation between the radiation darkening pattern and the scattering pattern. Two fine lines were cut on one of the surfaces of specimen G II_3. Before any treatment the plate was clear. After pile irradiation

(1.7×10^{18} $n°$ cm.$^{-2}$) the crystal appeared in transmitted light as in the photograph of Fig. 2*a*. Fig. 2*b* shows the appearance after heating at 700° C. for 24 hours. The radiation color is bleached by this treatment and the prismatic scattering regions are apparently induced as in an unirradiated crystal. A comparison of the two photographs shows that the regions of radiation coloring correspond with those which scatter light preferentially. The experiment also shows that previous neutron irradiation does not prevent the subsequent formation of light scattering centers.

A similar specimen was etched in 10% hydrofluoric acid for 12 hours

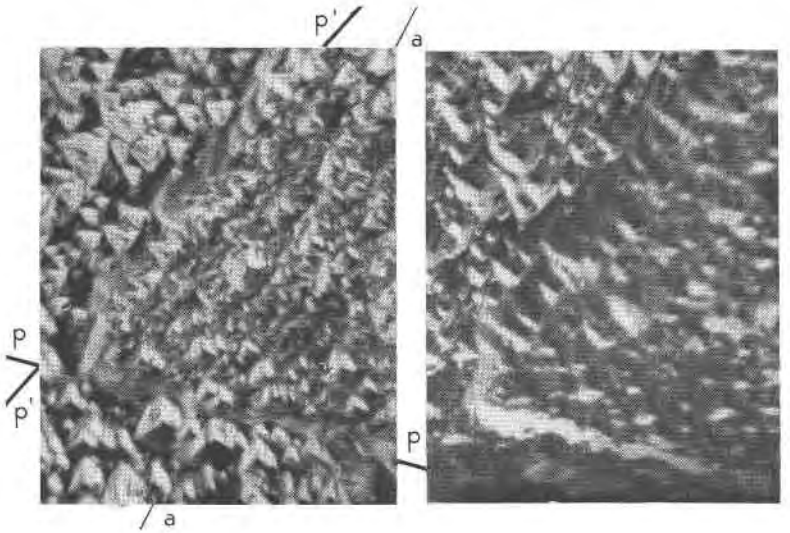

FIG. 3. Photographs of the 0001 surface of specimen G II_4 after etching in 10% HF. (Left) Focused on the surface within the prism boundary p-p and p′-p′ (a-a is *a*-axis direction. (Right) Focused on the surface outside the prism. 885×.

after having been heated at 700° C. Figure 3 shows a photograph of the etching pattern using a magnification (×400) such that only one prism surface appears in the field of view. It was also found, by focussing on to the surface of the crystal first within and then outside the prism, that more material had been removed from within the prism. The photographs show that there is a greater density of etch pits within the prism than outside it.

G.E.C. Type G III

Pile irradiation produces a non-uniform darkening in which triangular prismatic regions are evident but they are smaller and less geometrically exact than those produced in G II specimens. Figure 4 is a photograph

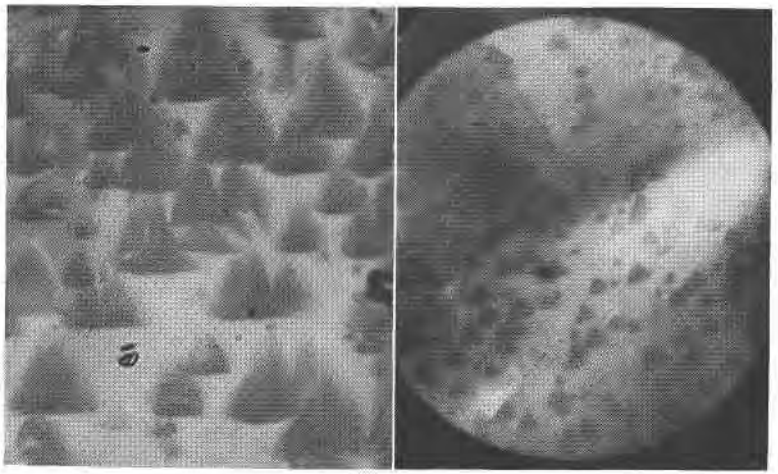

FIG. 4. (Left) Specimen G III_3 after neutron irradiation (1.7×10^{18} $n°$ cm.$^{-2}$) viewed in the c-axis direction. 148×.

FIG. 5. (Right) Specimen G III_3 after heating at 700° C. for 24 hours, viewed in the c-axis direction. 40×.

of specimens G III, after a neutron dose of 1.7×10^{18} $n°$ cm.$^{-2}$. It will be seen that there are light streaks running from the apices to the centers of the triangular regions.

In the case of G III_4, the only specimen of this type which has been heat treated, light is scattered from most of the crystal but there are prisms of approximately triangular cross-section within which there is a preferentially *lower* density of scattering centers (Fig. 5).

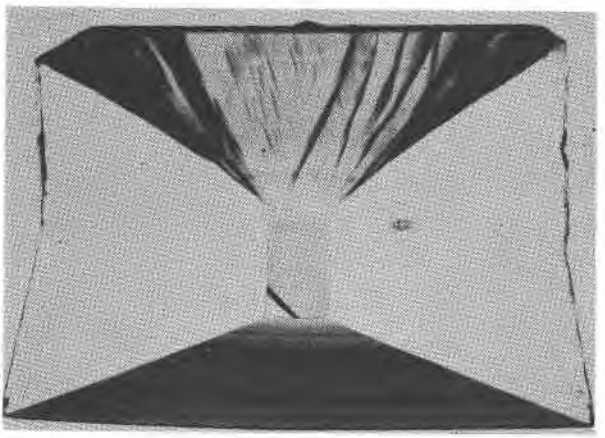

FIG. 6. Sawyer Products crystal viewed in the Y direction after neutron irradiation (1.7×10^{18} $n°$ cm.$^{-2}$). 3×.

Y-Bar Crystals (Sawyer Products)

The specimens were cut from the same crystal at right angles to the Y direction. In each case, the only region in which noticeable scattering was produced by heat treatment was in the slow growing X direction. The scattering density appeared fairly uniform throughout this region although there was a tendency for the density to be greater in laminated regions perpendicular to the growth direction and separated by about 0.05 cm. The effect of pile irradiation on unheated specimens is as shown in Fig. 6. Although the darkening in some parts of the crystal is extremely non-uniform, there are only slight variations in the part of the

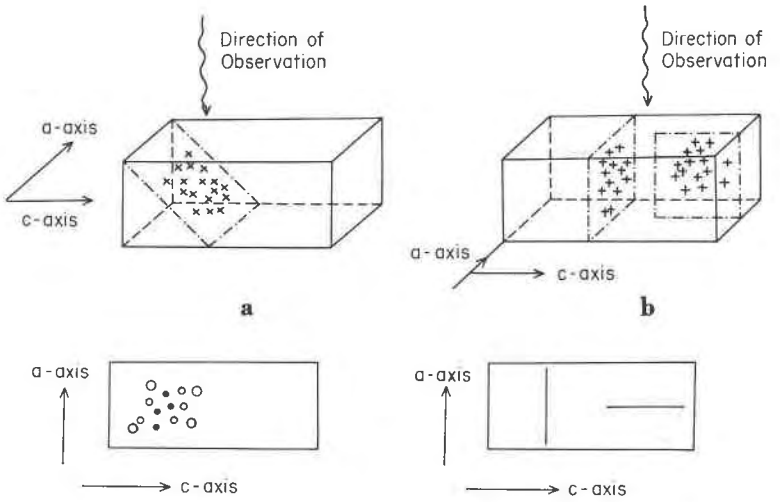

FIG. 7. Precipitation planes viewed (a) as planes, and (b) as lines in synthetic quartz.

crystal in which scattering centers are produced. Both Hale (1957) and Cohen (1957) have found similar patterns in the original Y bar crystals grown at the Clevite Research Center.

OBSERVATIONS OF INDIVIDUAL SCATTERING CENTERS IN G.E.C. TYPE G I SPECIMENS

Individual scattering centers were most clearly detected in Type G I specimens, from which, as described above, there was a relatively low intensity of scattered light. It is convenient to divide into two the distribution of centers revealed by the examination with the 4 mm. dark field objective (this was found to give optimum viewing conditions).

(a) Scattering centers grouped in apparently open clusters on planes not containing the direction of viewing (Fig. 7). It was found impossible to bring all the centers in a

given cluster into focus at once. This indicated that the centers were located at different depths within the crystal. If the specimen was moved slowly in the direction of observation the imaginary line, along which the centers were in focus, moved across the cluster. This type of grouping occurred principally in specimens heated for only a short time at comparatively low temperatures (700° C).

(b) Scattering centers grouped into planes containing the direction of viewing (Fig. 7). These centers are in planes which are viewed edge on so that they appear as lines which remains in focus when the specimen is moved in the direction of view. For a given specimen position the centers in focus were seen against a blurred background arising from the out of focus centers above and below the focal plane. Groups of this kind occurred most frequently in the higher temperature heat treatments.

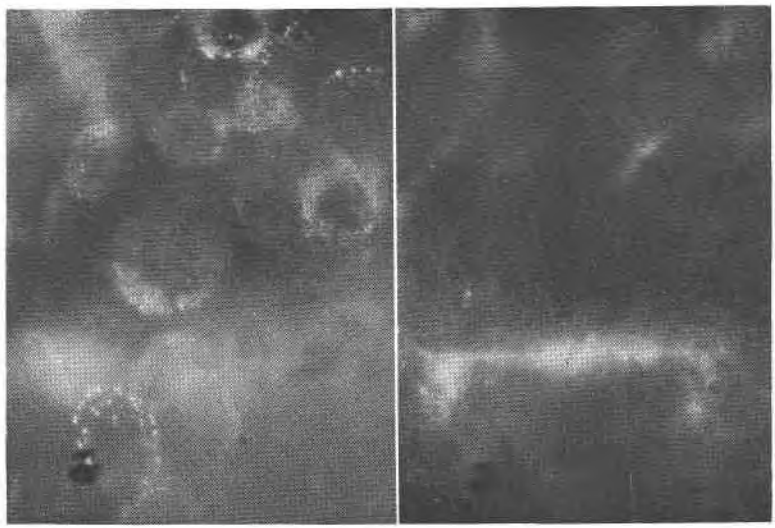

FIG. 8. Photographs of precipitation planes and particles in specimen G I_{16} viewed in an *a*-axis direction with the *c*-axis parallel to the base of each plate. 700×.

A particular region of specimen G I_{17} was examined both after a light and a subsequent heavy heat treatment. After the first heating (1 hour at 700° C.) a large number of open groups (*a*), and a few weak lines (*b*) were noticeable. After the second heat treatment (72 hours at 900° C.) the original lines were re-identified but were found to have extended much further into the crystal. It was not possible to re-identify the clusters which were much less apparent than after the heating at 700° C. These observations indicate that the two groups of centers are not only distinguished by their orientation but also by their condition of formation.

Photographs of both types of grouping are shown in Fig. 8.

Orientation of Planes

The orientation of type (*b*) clusters could be readily found by measuring the angle of the line relative to the *c*-axis. These angles (see Fig. 7) 0°; 36° 50′; and 90°. This data is summarized on the stereographic projection of Fig. 9.

The orientation of the planes containing the open clusters was found by determining the Cartesian co-ordinates of the in focus centers in a cluster. We suppose that for the first observation the focal plane of the microscope is in the crystal at $z_1=0$. The (x,y) co-ordinates were measured directly using the two micrometers on the stage, or by photographing and measuring the in focus spots on the plate. The microscope was then racked a distance d and a second set of (x,y) measurements taken (either directly or photographically) on the in focus spots at a depth in the crystal $z_2=nd$ (where n is the refractive index). The procedure was

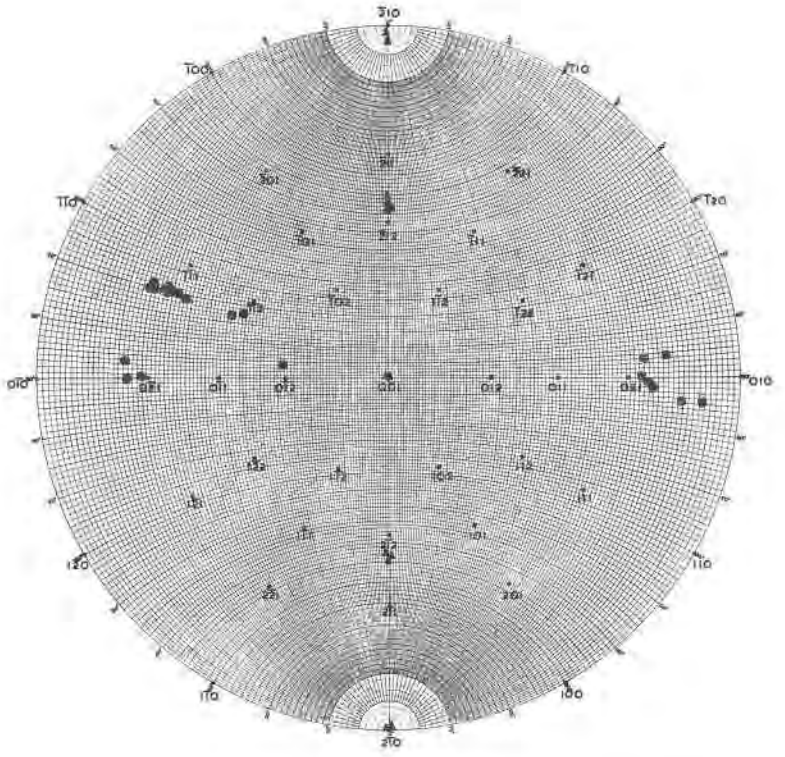

FIG. 9. Stereographic projection showing the directions of planes of scattering particles. ● planes seen as planes; ▲ planes seen as lines; • reference points of the projection.

repeated for various depths in the crystal $z_j = n(j-1)d$, for $j = 3,4$ etc. Using the 4 mm. objective the value of d used was 3×10^{-4} cm., giving for example $z_{11} = 46.2 \times 10^{-4}$ cm., with an uncertainty of $\pm 2 \times 10^{-4}$ cm. The errors in the determination of the (x,y) co-ordinates were about $\pm 1 \times 10^{-4}$ cm.

The measured co-ordinates for the scattering centers in a cluster were taken in groups of three and the values A, B, C of the equation of the plane: $Ax + By + Cz = 1$ were determined. From the mean values of A:B:C determined for a given cluster the $(hk \cdot l)$ hexagonal indices for the plane of the cluster were found using the relation:

$$(hk \cdot l) \equiv \mathrm{A}; \qquad \frac{\mathrm{B}\sqrt{3} - \mathrm{A}}{2} : 1 \cdot 100\ \mathrm{C}$$

This data about orientation of planes containing scattering centers is also summarized in the stereographic plot of Fig. 9.

Rate of Production of Scattering Centers

From the transmission (T) measured with the spectrophotometer we have calculated the total light removal coefficient (Σ) from the equation:

$$T = (1 - R)^2 e^{-\Sigma x}$$

where R is the fractional reflection loss from a specimen before heat treatment and x is the specimen thickness. This relation is the approximation to equation (7) of Bastin *et al.* (1959) when $R^2 e^{-2\Sigma x} \ll 1$.

It will be seen from Fig. 10 that Σ increases with length of heat treatment and finally reaches a saturation value. The rate of increase of Σ is temperature dependent; the rate increasing with increasing temperature.

The saturation value of Σ does not vary appreciably with the heating

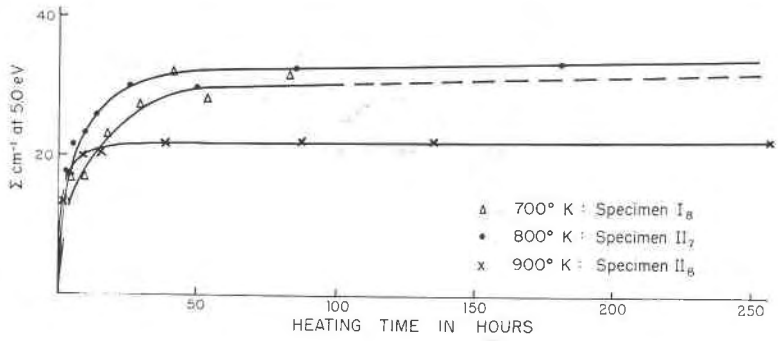

Fig. 10. Saturation of light scattering with heat treatment for specimens of type G II.

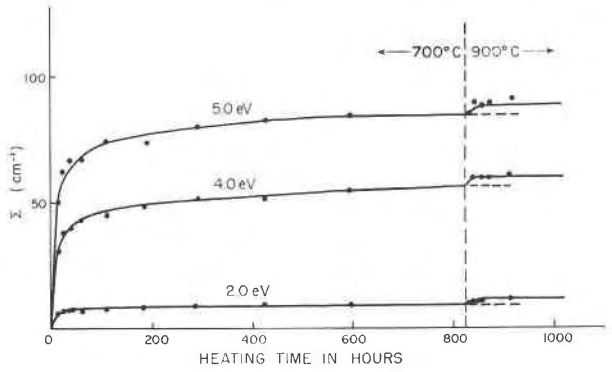

FIG. 11. Variation of Σ for specimen G II_2 heated first at 700° C. and then at 900° C.

temperature. In Fig. 11 results of heating specimen G II_2 for 830 hours at 700° C. are shown and a value of $\Sigma = 57$ cm.$^{-1}$ was reached at a wavelength of 3090 Å. Subsequent heating at 900° C. caused only a small increase in Σ to 61 cm.$^{-1}$ at the same wavelength.

The results of integrating sphere and transmission measurements are shown in Fig. 12. With the exception of the absorption band at 4200 Å which only occurred in a few specimens, the two sets of measurements indicate that most of the loss of light in the transmission experiments is due to scattering and not absorption. Determination of the coefficient Σ from spectrophotometer measurements thus gives a convenient measure of the light scattering within a specimen.

In order to determine whether the size of scattering particles is dependent on the heat treatment we have plotted Σ as a function of wavelength λ on logarithmic scales, for a crystal after a short and also a long high temperature heat treatment. The results are shown in Fig. 13. It will be seen that the wavelength dependence of log Σ has not changed markedly, indicating that although the amount of scattered light has increased, the mean size of the scattering particles has not changed significantly.

The saturation value of Σ was found to be highest in the G III and lowest in the G I specimens. We have already referred to the different concentrations of Al impurity in these crystals (Table I). The saturation values of Σ are also given in that table from which it is clear that Σ increases with increasing Al concentration.

DISCUSSION OF RESULTS

The results which have been described above may be summarized as follows:

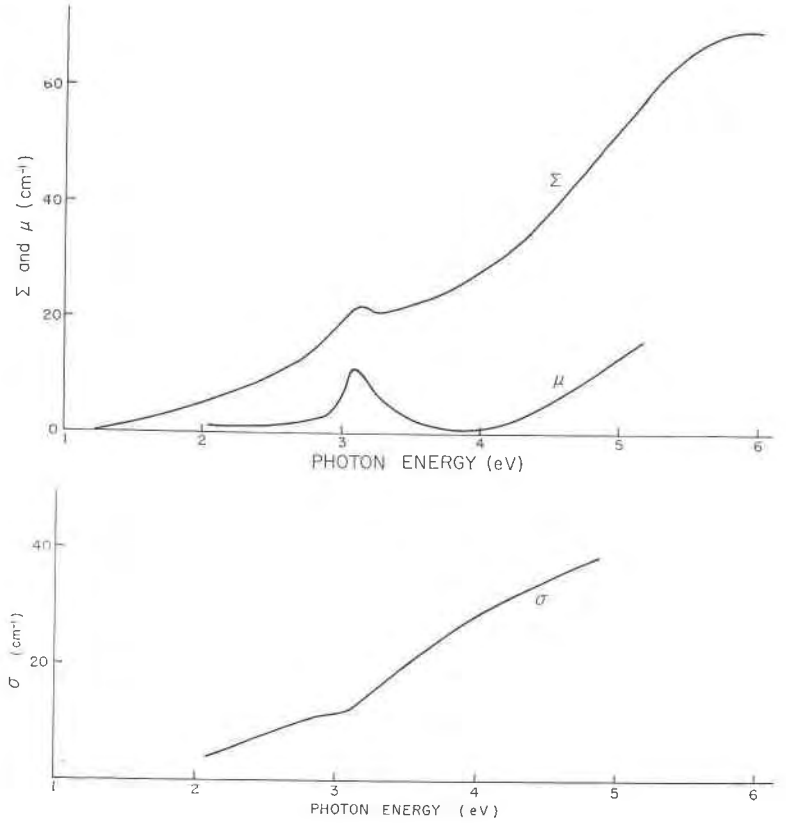

FIG. 12. Integrating sphere and transmission measurements for Specimen G III$_4$ after heating at 700° C. for 20 hours, (above) Σ from spectrophotometer measurements, and coefficients of absorption μ from integrating sphere measurements. (below) Coefficients of scattering σ calculated as the difference $\Sigma - \mu$.

(*a*) with the exception of growth in the *c*-axis directions in Y-bar crystals, heat treatment of synthetic quartz produces particles which scatter light.
(*b*) the spatial distribution of these particles varies in crystals grown under different conditions.
(*c*) the amount of scattering reaches a saturation value which takes longer to reach at lower temperatures.
(*d*) the saturation value is higher in specimens with high Al concentration.

We first consider two possible mechanisms for the formation of scattering particles. In subsequent sections we discuss the kinetics in relation to the second mechanism and the spatial orientation of the centers.

Bubble Mechanism

All the crystals were grown from aqueous solutions. It is possible,

as has been shown to be the case with some alkali halides, that the crystals contain cavities which are filled or partially filled, with aqueous growth solution. We may suppose that at high enough temperatures, the bubbles develop sufficient pressure to fracture the surrounding crystal which then causes light to be scattered.

Brown and Thomas (1956) observed light scattering which they attributed to this mechanism during their examination of some of the earlier and poorer quality synthetic quartz. In their case, however, the cavities were visible before heat treatment and the specimens also had

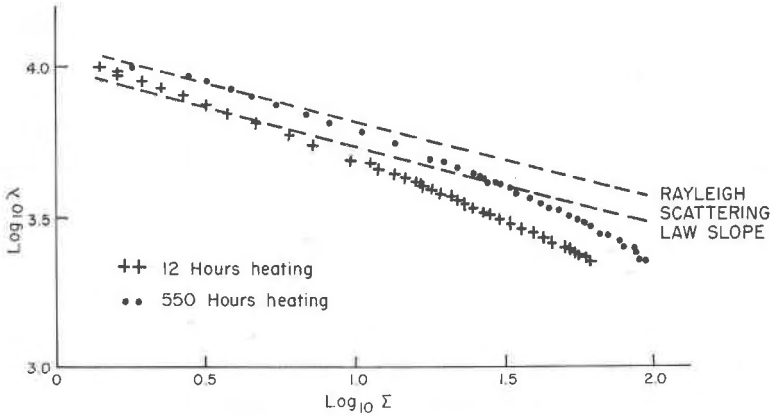

FIG. 13. Logarithmic plots of Σ as a function of wavelength for specimen G I_{18} after heating at 700° C.

a strong absorption band at 3μ corresponding to the O-H vibration in water. Neither of these features was observed in our specimens, although there was evidence of a weak (≈ 1 cm.$^{-1}$) absorption band at 2.8μ corresponding to isolated O-H vibrations.

Apart from the absence of spectroscopic evidence for the presence of water in the crystals examined, there is a further difficulty about the bubble mechanism. There will be a temperature at which most of the bubbles develop sufficient pressure to cause the surrounding crystal to fracture. We should expect that after heating at this temperature the amount of scattered light would have greatly increased, although the effect would presumably occur over a range of heating temperatures, corresponding to the range of filling of the cavities in the original crystal. Thus the "saturation" value reached at any temperature would be very temperature dependent, which is contrary to what was observed (see Fig. 11).

Precipitation Mechanism

In this mechanism we assume that there are precipitation sites in the

crystals at which impurity atoms are precipitated, and that the rate of precipitation is mainly governed by the thermally activated migration of the impurity atoms to these sites. The occurrence of regions of high scattering power in regions of strong radiation darkening indicates that Al may be the impurity involved, since there is considerable evidence that radiation darkening is associated with the presence of Al. Item (*d*) in the summary of results could also be accounted for if the impurity being precipitated were Al. The assignment may not be unique, however, for there may be other impurities which increase when the Al concentration increases.

Evaluation of the Activation Energy for the Precipitation Mechanism

Let N be the number of atoms per unit volume which at the start of the process are capable of being precipitated. The rate of precipitation at any time will be related to some function of N and also of n_t the number of atoms per unit volume which by time t have been precipitated. Thus:

$$\frac{dn_t}{dt} = Af(N, n_t)e^{-\epsilon/kT} \tag{1}$$

where $f(N, n_t)$ is a function of N and n_t, and A is a constant which may be specimen dependent.

As a measure of the light scattering we use the value of the coefficient Σ at a photon energy of 5 eV (2470 Å). Σ will be a function of the number of precipitation centers and of the size of the individual particles. We assume that the concentration of precipitation centers is a constant for a given crystal and that:

$$\Sigma_t = \alpha n_t^x \tag{2}$$

where α and x are constants. Thus:

$$\frac{dn_t}{dt} = \left(\frac{1}{\alpha}\right)^{1/x} \cdot \frac{1}{x}\, \Sigma^{1/x-1}\, \frac{d\Sigma_t}{dt}. \tag{3}$$

From (1) using results obtained at two temperatures on the same specimen and following Overhauser (1953) we can write, independently of the form of $f(N, n_t)$, that:

$$\epsilon = \frac{k}{\left(\frac{1}{T_2} - \frac{1}{T_1}\right)} \ln \left[\left(\frac{\partial n_t}{\partial t}\right)T_1 \Big/ \left(\frac{\partial n_t}{\partial t}\right)T_2\right] \tag{4}$$

where the slopes $(\partial n_t/\partial t)_T$ have to be evaluated for the same value of t. If we measure the slopes at this value of t, using (3) we may write equation (4) as:

$$\epsilon = \frac{k}{\left(\frac{1}{T_2} - \frac{1}{T_1}\right)} \ln \left[\left(\frac{\partial \Sigma_t}{\partial t}\right) T_1 \Big/ \left(\frac{\partial \Sigma_t}{\partial t}\right) T_2 \right] \tag{5}$$

The results which may be used to evaluate ϵ from equation (5) must all refer to one specimen. Experimentally it is difficult to determine both slopes accurately. Two series of values of ϵ determined in this way on two specimens gave a mean of 0.9 eV, but the values ranged from 0.6 to 1.3 eV.

In order to improve the accuracy it is necessary to use results obtained on pairs of specimens, each member of a pair being heated at a different temperature. However, to deduce ϵ from the results we have to make more specific assumptions about the form of $f(N, n_t)$. We assume first that the rate of precipitation is proportional to the number of unprecipitated atoms. Thus:

$$\frac{dn_t}{dt} = (N - n_t) A e^{-\epsilon/kT} \tag{6}$$

where A is a constant which is related to the concentration of precipitation sites. Since $n_t = 0$ at $t = 0$ this equation may be integrated to give:

$$\ln \left(1 - \frac{n_t}{N}\right)^{-1} = tAe^{-\epsilon/kT}$$

or

$$\ln \left(1 - \frac{\Sigma_t{}^{1/x}}{\Sigma_\infty{}^{1/n}}\right)^{-1} = tAe^{-\epsilon/kT} \tag{7}$$

where Σ_∞ corresponds to saturation conditions in which all N atoms are precipitated. If we now determine the time t_1 needed at temperature T_1 for one specimen to reach a particular value of Σ_t/Σ_∞ and then the time t_2 for another specimen to reach the same value of this ratio at temperature T_2, we can calculate ϵ provided that A does not differ significantly between the two specimens. We do not have to specify x, and (from equation (7)) ϵ is given by:

$$\epsilon = \frac{k}{\left(\frac{1}{T_1} - \frac{1}{T_2}\right)} \ln \left(\frac{t_1}{t_2}\right) \tag{8}$$

We have used a value of $\Sigma_t/\Sigma_\infty = 0.8$ and following the above procedure measurements on 11 crystals (covering a temperature range 700°–900° C. and a corresponding time range 1–500 hours) give a value of $\epsilon = 1.15 \pm 0.3$ eV.

We now consider a modification of the above assumptions. If the scattering particles grow continuously throughout the process the number

of sites available for precipitation will increase with time, and will be proportional to the surface area of the particles. This surface area will be proportional to $n_t^{2/3}$ if the particles keep the same shape, so that equation (6) becomes:

$$\frac{dn_t}{dt} = (N - n_t)n_t^{2/3}A'e^{-\epsilon/kT} \tag{9}$$

where A' is a constant which is again related to the concentration of precipitation sites, and may thus be specimen dependent. Equation (9) gives on integration:

$$tA'e^{-\epsilon/kT} = \frac{1}{N^{2/3}}\left\{\ln\left[\frac{(n_t^{2/3}+N^{1/3}n_t^{1/3}+N^{2/3})^{1/2}}{(N^{1/3}-n_t^{1/3})}\right] + \sqrt{3}\tan^{-1}\left[\frac{2n_t^{1/3}+N^{1/3}}{\sqrt{3}N^{1/3}}\right] - \frac{\pi}{2\sqrt{3}}\right\}$$

which may be written as:

$$\begin{aligned} tA'e^{-\epsilon/kT} &= \frac{1}{N^{2/3}}f\left(\frac{n_t}{N}\right) \\ &= \left(\frac{\alpha}{\Sigma_\infty}\right)^{2/3x}f\left(\frac{\Sigma_t}{\Sigma_\infty}\right) \end{aligned} \tag{10}$$

Thus choosing a value of Σ_t/Σ_∞ which is obtained by conditions (T_1 t_1) in one specimen and (T_2 t_2) in another, we have by analogy to equation (8):

$$\epsilon = \frac{k}{\left(\frac{1}{T_1}-\frac{1}{T_2}\right)}\left[\ln\left(\frac{t_1}{t_-}\right) + \frac{2}{3x}\ln\left(\frac{\Sigma_{\infty_2}}{\Sigma_{\infty_1}}\right)\right] \tag{11}$$

In order to evaluate ϵ we have to make a specific assumption about x. If the dimensions of the scattering particle are small compared with the wavelength of the light, and if the attenuation of the wave within the particle is small, the scattering per particle is proportional to the 6th power of the radius r (i.e. $\Sigma_t \propto n_t^2$ or $x=2$, since $r^6 \propto V^2$ and $V \propto n_t$) for a fixed number of precipitation centers.

Using this procedure we find a value of $\epsilon = 1.08 \pm 0.10$ eV. This value does not differ appreciably from the previous value. It is interesting that this more detailed treatment gives a significant reduction in the spread of the values obtained for ϵ.

Values of ϵ for some impurities in quartz have been found from the study of the ionic conductivity arising from added ions. Such measurements have been made by Vogel and Gibson (1950), Verhoogen (1952), and Kirton (1960). The values found are all about 1 eV, but the accuracy is not sufficient to identify our value of 1.08 eV with that for any particular impurity.

Spatial Distribution

(*a*) Distribution of individual particles.

Figure 8 together with measurements of the co-ordinates of individual particles show that there are planes of area 10^{-6}–10^{-5} cm.^{2} on which the particles are located. Of these the 001, $\bar{2}10$ and $2\bar{1}0$ planes have been identified as simple crystallographic planes with low Miller indices. The reason for the arrangement of particles in this way is not clear, but it is possible that each plane is some kind of two dimensional defect. The intersection of dislocations with these defects could provide the precipitation sites for scattering particles.

(*b*) Large scale distribution of precipitate.

In general it is not clear why some regions give relatively dense precipitation on heating while other regions (*e.g. c*-axis growth direction of Sawyer crystals) show no measurable precipitation. Further it is not clear why precipitation should occur in synthetic and not in natural quartz.

In specimens of type G I, G II (see Fig. 2*b*) and in the slow X growth direction of Sawyer crystals (see Fig. 6), macroscopic laminae are found parallel to the growth surface. This laminated distribution would be expected if growth conditions were variable, or perhaps if the deposition of impurity were a co-operative phenomenon.

In G II type specimens the prismatic regions are of interest. No reasons can be given for the exact form of the prisms although trigonal symmetry in the basal plane would be expected and the regular axial propagation of the prism in the growth direction is also reasonable. Within the prisms both preferentially high precipitation and radiation darkening is observed. The results suggest Al as a possible constituent of the precipitate. This suggestion agrees with the correlation with radiation darkening since the latter has been attributed to Al by a number of workers (see for example E. W. J. Mitchell and E. G. S. Paige 1955). The presence of a high etch pit density on the exposed basal planes of the prisms (see Fig. 3) indicates a high density of defects within the prisms, a condition which might be expected to facilitate precipitation.

Acknowledgments

We should like to thank Professor R. W. Ditchburn for his interest in this work, and we are grateful to Mr. L. A. Thomas and Mr. C. S. Brown of the G.E.C. Research Laboratory, Wembley, Middlesex for the provision of specimens and for helpful discussions. It is also a pleasure to acknowledge the comments of Dr. A. J. Cohen of the Mellon Insti-

tute, Pittsburgh with whom some of the results were discussed, and Sawyer Products, Cleveland for the loan of a Y-bar crystal.

References

Bastin, J. A., Mitchell, E. W. J., and Whitehouse, J., *Brit. Journ. App. Phys.*, **10,** 412, 1959.

Brown, C. S., and Thomas, L. A., *Proc. Inst. Elect. Eng.*, **104,** 174, 1956.

Cohen, A. J., Private communication. 1957.

Bechmann, R., and Hale, D. R., *Journal of Brush Electronics Co.*, **4,** No. 1, 1, 1955, and Hale, 1957. Private communication. 1960.

Kirton, J., Ph.D. thesis, Reading University, 1960.

Mitchell, E. W. J., and Paige, E. G. S., *Phil. Mag.*, **46,** 1353, 1955.

Overhauser, A. W., *Phys. Rev.*, **90,** 393, 1953.

Verhoogen, J., *Amer. Min.*, **37,** 637, 1952.

Vogel, R. C., and Gibson, G., *J. Chem. Phys.*, **18,** 490 and 1094, 1950.

Manuscript received November 15, 1960.